MICROSTRUCTURE, MECHANICAL PROPERTIES, AND CORROSION BEHAVIOR OF CRYOROLLED LOW CARBON STEEL SUBJECTED TO HEAT TREATMENT

KANCHANA MOTHAM

UNIVERSITI SAINS MALAYSIA

2018

MICROSTRUCTURE, MECHANICAL PROPERTIES, AND CORROSION BEHAVIOR OF CRYOROLLED LOW CARBON STEEL SUBJECTED TO HEAT TREATMENT

by

KANCHANA MOTHAM

Thesis submitted in fulfilment of the
requirements for the degree of
Master of Science

December 2018

ACKNOWLEDGEMENT

Deep gratitude and sincere thanks that come deeply from my heart to all who supported me and make me across all the struggling to complete this thesis. Firstly, I would like to express my thanks and gratitude to University Science Malaysia and School of Materials and Mineral Resources Engineering for providing me sufficient equipment to complete this research. I would like to give a great appreciation to my beloved supervisor, Dr. Anasyida Abu Seman, for her excellent scientific guidance, inspiration, and trust. The door to her office was always open whenever I ran into a trouble spot or had a question about my research or writing. Without her right direction, it is impossible for me to complete my master program and this thesis. I also would like to thank deeply to my co-supervisor, Professor Dr. Zuhailawati Bt. Hussain, who always there for me. Nevertheless, I would like to express my sincere gratitude to my Thailand supervisor, Dr. Sunisa Khamsuk of Burapha University, for her help and supports. My appreciation also goes to all staff and technician of School of Materials and Mineral Resources Engineering, who have directly or indirectly involved in my research, especially Mr. Zul, Mr. Shafiq, Mr. Farid and Mr. Shahril. Without their passionate participation and input, the research could not have been successful. Special thanks and gratefully acknowledge to AUN/SEED-Net, JICA for giving me the opportunity and financial support to pursue my education. Thank you also to AUN/SEED-Net JICA officers for their excellent service. Finally, I must express my very profound gratitude to my parents and to my senior for providing me with unfailing support and continuous encouragement throughout my years of study and through the process of researching and writing this thesis. This accomplishment would not have been possible without them. Thank you.

TABLE OF CONTENTS

		Page
ACKNOWLEDGEMENT		ii
TABLE OF CONTENTS		iii
LIST OF TABLES		viii
LIST OF FIGURES		x
LIST OF ABBREVIATIONS		xiv
LIST OF SYMBOLS		xvi
ABSTRAK		xvii
ABSTRACT		xix
CHAPTER ONE: INTRODUCTION		
1.1	Background Research	1
1.2	Problem statement	5
1.3	Objectives	6
1.4	Scope of research	7
CHAPTER TWO: LITERATURE REVIEW		
2.1	Introduction	8
2.2	Steel	8
2.3	Low Carbon Steel (LCS)	10
2.3.1	Phase diagram of steel	12
2.4	Strengthening Mechanism	15
2.5	Severe Plastic Deformation (SPD)	18
2.6	Cryorolling	21
2.7	Influence of processing parameter prior cryorolling	26
2.7.1	Influence of pre-heat treatment	26

2.7.2 Influence of soaking time in liquid nitrogen 30
2.7.3 Influence of thickness reduction during cryrolling 32
2.8 Effect of cryorolling on microstructure and mechanical properties 33
2.8.1 Influence of cryorolling on microstructure 33
2.8.2 Influence of cryorolling on crystallite size and lattice strain 35
2.8.3 Influence of cryorolling on hardness properties 38
2.8.4 Influence of cryorolling on tensile properties 40
2.8.5 Influence of cryorolling on fracture behavior 43
2.9 Influence of post annealing 44
2.10 Corrosion 47
2.10.1 Principles of corrosion 47
2.10.2 Corrosion mechanism of steel 48
2.10.3 Corrosion testing and measurement 50
2.10.4 Corrosion behavior of low carbon steel 54

CHAPTER THREE: MATERIALS AND METHODS

3.1 Introduction 56
3.2 Material 56
3.3 Chemical 57
3.4 Sample preparation, annealing and cryorolling 58
3.4.1 Pre-heat treatment 60
3.4.2 Selection of soaking time in liquid nitrogen prior to cryorolling 61
3.4.3 Selection of pre-annealing temperature and soaking time prior to cryorolling process 62
3.4.4 Selection of percentage thickness reduction on cryorolled low carbon steel 64
3.4.5 Selection of post annealing temperature after cryrorolling 64
3.5 Materials characterization 65

3.5.1 Chemical composition analysis 65
3.5.2 Optical microscope attached with image analyzer (OM-IA) 66
3.5.3 Metallographic preparation for optical microscope 66
3.5.4 Scanning electron microscopy (SEM) 67
3.5.5 Electron backscatter diffraction (EBSD) 68
3.5.6 X-ray Diffraction (XRD) analysis 68
3.5.7 Microhardness test 70
3.5.8 Tensile test 71
3.5.9 Potentiodynamic polarization corrosion test 72

CHAPTER FOUR: RESULTS AND DISCUSSION

4.1 Introduction 76
4.2 Characterization of as received low carbon steel 76
4.2.1 Chemical composition analysis of as received low carbon steel 76
4.2.2 Microstructure analysis of as received material 78
4.2.3 Phase analysis of as received material 79
4.3 Preliminary study of low carbon steel before cryorolling 80
4.4 Effect of pre-heat treatment and soaking time prior cryorolling on low carbon steel 86
4.4.1 Microstructural analysis of low carbon steel after annealed and annealed followed by cryorolling at various annealing temperatures 87
4.4.2 X-ray diffraction analysis of low carbon steel after annealed and annealed followed by cryorolling at various annealing temperatures 92
4.4.3 Microhardness of low carbon steel after annealed and annealed followed by cryorolling at various annealing temperatures 94
4.4.4 Tensile properties of low carbon steel after annealed and annealed followed by cryorolling at various annealing temperatures 95

4.4.5 Fracture surface morphology of low carbon steel after annealed and annealed followed by cryorolling at various annealing temperatures 98

4.5 Effect of thickness reduction on cryorolled of low carbon steel 102

4.5.1 Microstructural analysis of cryorolled low carbon steel at various thickness reductions 102

4.5.2 EBSD analysis of cryorolled low carbon steel at various thickness reductions 108

4.5.3 X-ray diffraction of cryorolled low carbon steel at various thickness reductions 111

4.5.4 Hardness of cryorolled low carbon steel at various thickness reductions 114

4.5.5 Tensile properties of cryorolled low carbon steel at various thickness reductions 116

4.5.6 Fractural morphologies of cryorolled low carbon steel at various thickness reductions 119

4.5.7 Corrosion behaviour of cryorolled low carbon steel at various thickness reductions 121

4.6 Effect of post annealing in various thickness reductions after cryorolling 124

4.6.1 Microstructure analysis of 70% and 90% cryorolled low carbon steel at various post annealing 124

4.6.2 X-ray diffraction of 70% and 90% cryorolled low carbon steel at various post annealing 127

4.6.3 Hardness of 70% and 90% cryorolled low carbon steel at various post annealing 131

4.6.4 Tensile properties of 70% and 90% cryorolled low carbon steel at various post annealing 133

4.6.5 Corrosion behaviour of 70% and 90% cryorolled low carbon steel at various post annealing 137

CHAPTER FIVE: CONCLUSIONS AND SUGGESTION FOR FUTURE WORK

5.1 Conclusions 141

5.2 Suggestions for future research 143

REFERENCES 144

LIST OF TABLES

		Page
Table 1.1	Mechanical properties of various steel and its application (Singh, 2016)	3
Table 2.1	Compositions of low carbon steel, mechanical property, and typical applications for various low carbon steel (Rakhit, 2013, Altan and Tekkaya, 2012)	11
Table 2.2	Microstructure phase in iron-iron (Hasan, 2016)	13
Table 3.1	Properties of liquid nitrogen (Flynn, 2004)	57
Table 4.1	Theoretical chemical composition of low carbon steel (ASTM, 2016)	77
Table 4.2	Chemical composition of as-received low carbon steel	77
Table 4.3	Grain aspect ratio of cryorolled low carbon steel at various soaking time	85
Table 4.4	Grain aspect ratio of low carbon steel after annealed and annealed followed by cryorolling	90
Table 4.5	Crystallite size and lattice strain of low carbon steel after annealed and annealed followed by cryorolling at various annealing temperatures	93
Table 4.6	Grain aspect ratio of cryorolled low carbon steel at various thickness reduction	107
Table 4.7	Full width at haft maximum intensity of cryorolled low carbon steel at various thickness redcution	112
Table 4.8	Strain hardening coefficient of cryorolled low carbon steel at various thickness reduction	119
Table 4.9	Ecorr, Icorr, and corrosion rate of cryorolled low carbon steel at various thickness reduction	123
Table 4.10	Grain aspect ratio of 70% and 90% cryorolled low carbon steel at various post annealing	127

Table 4.11 Full width at half maximum intensity of 70% and 90% cryorolled low carbon steel at various post annealing 131

Table 4.12 Corrosion potential, current density, and corrosion rate of 70% and 90% cryorolled low carbon steel at various post annealing 140

LIST OF FIGURES

		Page
Figure 1.1	Light vehicle metallic material trend in north america (Singh, 2016)	2
Figure 2.1	Classification of metallic (Shaymaa, 2012)	9
Figure 2.2	Iron-Iron carbide phase diagram (Gendy, 2007)	14
Figure 2.3	Phase transformation via annealing from austenite area (Shah, 2009)	15
Figure 2.4	Rolling process (Dieter, 1988)	16
Figure 2.5	Schematic process of cryorolling (Yu et al., 2016)	22
Figure 2.6	Schematic diagram of microstructural evolution occurs during severe plastic deformation. (a) homogeneous distribution of dislocation, (b) elongated cell formation, (c) dislocation obstructed by sub-grain boundaries, (d) destruction of elongated sub-grains and (e) reorientation of sub-grain boundaries and development of UFG structures (Mishra et al., 2005)	23
Figure 2.7	Engineering stress−strain curves of Al6061 alloy in different conditions (Abbasi-Baharanchi et al., 2017)	25
Figure 2.8	The influence of annealing temperature on the tensile strength and ductility of a brass alloy (Callister and Rethwisch, 2011)	27
Figure 2.9	Microstructure of aluminium 6061 (a) Solution treated (ST) at 520℃ for 2 h and (b) Solution treated ST and 92% cryorolling	34
Figure 2.10	Microstructure of cryorolled Fe-36Ni after post annealing at 550℃ for (a) 5 minutes, (b) 10 minutes, (c) 15 minutes, and 30 minutes (Zheng et al., 2016b)	35
Figure 2.11	Full width at half maximum (FWHM) from XRD peak (Hammond, 2009)	36
Figure 2.12	Hardness value comparison between cold rolled and cryorolled in different thickness reduction (Paper and Delhi, 2016)	39
Figure 2.13	Stress-strain result for different percentage reduction for (a) cryorolled samples and (b) cold rolled samples (Kumar and Kumar, 2017)	41

Figure 2.14	The effect of annealing on microstructure of cold worked metals, (a) cold worked, (b) after recovery, (c) after recrystallization, and (d) after grain growth (Khaira, 2013)	45
Figure 2.15	Corrosion mechanism for carbon steel in the electrolyte NaCl solution (Kunst et al., 2017)	49
Figure 2.16	Principal of anodic polarization scan (Davis, 2006)	53
Figure 2.17	Tafel plot from dynamic polarization measurement (McCafferty, 2010)	54
Figure 3.1	Flowchart of overall process	59
Figure 3.2	Annealing temperature profile	60
Figure 3.3	Process flow of low carbon steel at various soaking times in liquid nitrogen	62
Figure 3.4	Pre-annealing heat treatment at (a) 500℃, (b) 700℃, and (c) 900℃ for various soaking times	63
Figure 3.5	The RD surface side for optical observation	67
Figure 3.6	(a) Schematic diagram and (b) actual of potentiodynamic polarization set-up experiment	74
Figure 4.1	Optical microstructure of as-received material observed at a magnification of 200x (a) and 500x (b). F referred to Ferrite area and P referred to pearlite	78
Figure 4.2	X-ray diffraction of as received low carbon steel	79
Figure 4.3	Microhardness of cryorolled low carbon steel at various soaking times	82
Figure 4.4	Tensile strength and elongation of cryorolled low carbon steel at various soaking times	82
Figure 4.5	Microstructure of low carbon steel at soaking times of (a) 5, (b) 10, (c) 15, (d) 20, (e) 25 and (f) 30 minutes	84
Figure 4.6	Crystallite size and lattice strain of cryorolled low carbon steel at 50% thickness reduction at various soaking times	85
Figure 4.7	Microhardness of low carbon steel at various pre-annealing temperatures and soaking times	84

Figure 4.8	Microstructure after annealing at (a) 550°C, 60 minutes, (b) 750°C, 60 minutes, (c) 900°C, 15 minutes, (d) 550°C, 60 minutes followed by cryorolling, (e) 700°C, 60 minutes followed by cryorolling, and (f) 900°C, 15 minutes followed cryorolling	89
Figure 4.9	Grain size attribution of cryorolled low carbon steel annealed at (a) 550 ºC at 60 minutes, (b) 750 ºC at 60 minutes, and (c) 900 ºC at 15 minutes	91
Figure 4.10	X-ray diffraction pattern of low carbon steel after annealed and annealed followed by cryorolling at various annealing temperatures	92
Figure 4.11	Microhardness of low carbon steel after annealed and annealed followed by cryorolling at various annealing temperatures	95
Figure 4.12	Ultimate tensile strength of low carbon steel after annealed and annealed followed by cryorolling at various annealing temperatures	97
Figure 4.13	Yield strength of low carbon steel after annealed and annealed followed by cryorolled at various annealing temperatures	97
Figure 4.14	Elongation of low carbon steel after annealed and annealed followed by cryorolling at various annealing temperatures	98
Figure 4.15	Fracture morphology of annealed low carbon steel at various heat treatment, (a) 550°C at 60 minutes, (b) 750°C at 60 minutes, and (c) 900°C at 15 minutes	100
Figure 4.16	Fracture morphology of cryorolled low carbon steel annealed at, (a) 550°C at 60 minutes, (b) 750°C at 60 minutes, and (c) 900°C at 15 minutes	101
Figure 4.17	Microstructure of cryorolled low carbon steel at various thickness reductions (a, b) 50%, (c, d) 60%, (e, f) 70%, (g, h) 80%, and (i, j) 90%	104
Figure 4.18	SEM surface morphology of cryorolled low carbon steel at various thickness reductions (a, b) 50%, (c, d) 60%, (e, f) 70%, (g, h) 80% and (i, j) 90%	106
Figure 4.19	EBSD micrograph and rotation angle of cryorolled low carbon steel at various thickness reductions (a, b) 50%, (c, d) 70%, and (e, f) 90% (Black marks showed the bend directions)	109
Figure 4.20	Grain misorientation plot of cryorolled low carbon steel at various thickness reductions, (a) 50%, (b) 70%, and (c) 90%	110

Figure 4.21	X-ray diffraction of cryorolled low carbon steel at various thickness reductions	112
Figure 4.22	Crystalline size and lattice strain of cryorolled low carbon steel at various thickness reductions	114
Figure 4.23	Microhardness of cryorolled low carbon steel at various thickness reductions	115
Figure 4.24	Tensile properties and elongation of cryorolled low carbon steel at various thickness reductions	117
Figure 4.25	Stress-strain engineering curve of cryorolled low carbon steel at various thickness reductions	118
Figure 4.26	SEM fracture morphology of cryorolled low carbon steel at various thickness reductions, (a) 50%, (b) 60%, (c) 70%, (d) 80% and (e) 90%	121
Figure 4.27	Potentiodynamic polarization curve of cryorolled low carbon steel at various thickness reductions	123
Figure 4.28	Microstructure of 70% and 90% cryorolled low carbon steel at various post annealing (red marks are referred to recrystallization grain)	126
Figure 4.29	X-ray diffraction pattern of cryorolled low carbon steel at various post annealing (a) 70% reduction and (b) 90% reduction	129
Figure 4.30	Crystalline size and lattice strain of cryorolled low carbon steel at various post annealing (a) 70% reduction and (b) 90% reduction	130
Figure 4.31	X-ray diffraction of cryorolled low carbon steel at various post annealing (a) 70% reduction and (b) 90% reduction	132
Figure 4.32	Tensile strength, yield strength, and elongation of cryorolled low carbon steel at various post annealing (a) 70% reduction and (b) 90% reduction	135
Figure 4.33	Stress-strain curve of cryorolled low carbon steel at various post annealing (a) 70% reduction and (b) 90% reduction	136
Figure 4.34	Potentiodynamic polarization curve of cryorolled low carbon steel at various post annealing (a) 70% reduction and (b) 90% reduction	139

LIST OF ABBREVIATIONS

Al	aluminium
ARB	accumulative roll bonding
ASTM	American society for testing materials and minerals
BCC	body center cubic
C	carbon
CE	counter electrode
CG	coarse grain
Cr	chromium
CR	cryorolling
Cu	copper
EBSD	electron backscatter diffraction
ECAP	equal channel angular pressing
FESEM	field emission scanning electron microscope
Fe	ferrous
FCC	face center cubic
FWHM	full width at half maximum
HPT	high pressure torsion
IF	interstitial free steel
LCS	low carbon steel
Mn	manganese
NaCl	sodium chloride
Ni	nickel

OM	optical microscope
P	phosphorus
RE	reference electrode
S	sulfur
SCE	standard calomel electrode
SPD	server plastic deformation
Ti	titanium
TS	tensile strength
TWIP	twining induced plasticity steel
UFG	ultrafine grain
XRD	X-ray diffraction
YS	yield strength

LIST OF SYMBOLS

%	percentage
%C	percentage of carbon
%EL	elongation percentage
wt%	weight percentage
°C	degree celcius
D	spacing between the layer of atoms
HV	hardness Vickers
K	kelvin
kg	kilogram
min	minute
MPa	mega pascal
cm	centimeter
mm	milimeter
µm	micrometer
nm	nanometer
α	alpha ferrite
γ	austenite
λ	wavelength of ray
θ	angle between incident rays and surface of the crystal
T_m	melting temperature

MIKROSTRUKTUR, SIFAT-SIFAT MEKANIKAL DAN KELAKUAN KAKISAN KELULI KARBON RENDAH GELEKAN KRIO TERTAKLUK KEPADA RAWATAN HABA

ABSTRAK

Keluli karbon rendah telah digunakan secara meluas dalam pelbagai industri, tetapi kekuatan yang terhad menjadi halangan untuk membangunkan potensinya. Dalam tahun-tahun kebelakangan ini, bahan struktur berira halus telah dikaji, kerana ia dapat memberikan sifat mekanikal yang baik. Kajian semasa ini bertujuan untuk menghasilkan ira halus dalam keluli karbon rendah menggunakan gelekan krio dan mengkaji kesannya terhadap rawatan haba dan pengurangan ketebalan pada mikrostruktur, sifat mekanik dan kelakuan kakisan. Ciri-ciri mikrostruktur dan sifat-sifat mekanikal keluli karbon rendah dikaji menggunakan mikroskop optik (OM), mikroskop elektron pengimbasan (SEM), elektron bertaburan pembelauan (EBSD), pembelauan sinar-X(XRD), mikrokekerasan Vickers dan ujian tegangan. Keluli karbon rendah menjalani pra-penyepuhlindapan pada suhu 550°C, 750°C, dan 900°C selama 15, 30, 60 dan 120 minit dan diikuti dengan gelekan krio. Sampel pra-penyepulindap pada 550° C (60 minit) menunjukkan sifat mekanikal yang optimum dan ia dipilih untuk kajian pengurangan ketebalan yang berlainan; 50%, 60%, 70%, 80% dan 90%. Kekerasan dan kekuatan tegangan tertinggi dicapai pada 90% pengurangan dengan nilai masing-masing 208.5 Hv dan 826.5 MPa, saiz kristalit terkecil (38.16 nm) dan terikan kekisi tertinggi (20.58 x 10^{-4}). Rintangan kakisan berkurangan dengan pengurangan ketebalan. Pasca penyepuhlindapan pada suhu 450°C menunjukkan berlaku penghabluran pada pengurangan 90% dan telah mencapai

saiz ira halus dengan kekerasan dan kekuatan tegangan sebanyak 157.9 Hv dan 587.7 MPa.

MICROSTRUCTURE, MECHANICAL PROPERTIES, AND CORROSION BEHAVIOR OF CRYOROLLED LOW CARBON STEEL SUBJECTED TO HEAT TREATMENT

ABSTRACT

Low carbon steel has been extensively used in various industries, but its limited strength restricted the potential development in applications. In recent years, ultrafine grained (UFG) structural materials have been studied, because they are expected to provide superior mechanical properties. The present works aim at producing UFG in low carbon steel using cryorolling and investigated its effect on heat treatment and thickness reduction on microstructure, mechanical properties and corrosion behavior. The details of microstructural characteristics and mechanical properties of low carbon steel were investigated using optical microscope (OM), scanning electron microscope (SEM), electron back scattered diffraction (EBSD), X-ray diffraction (XRD), Vickers microhardness and tensile test. Low carbon steel underwent pre-annealing at 550°C, 750°C, and 900°C at 15, 30, 60 and 120 minutes followed by cryorolling. Sample treated at 550°C (60 minutes) shows the optimum properties and was chosen for futher investigation on different thickness reduction; 50%, 60%, 70%, 80% and 90%. The highest hardness and tensile strength attained at 90% reduction with the values of 208.5 Hv and 826.5 MPa respectively which result in the smallest crystallite size (38.16 nm) and highest lattice strain (20.58 x 10^{-4}). Corrosion resistance decreases with thickness reduction. Post-annealed at 450°C shows recrystallization state for 90% reduction and achieved ultrafine grain with hardness and tensile strength of 157.9 Hv and 587.7 MPa respectively.

CHAPTER ONE

INTRODUCTION

1.1 Background Research

Carbon steel is one of the most widely used materials in the industry. Low carbon steel contains lower than 0.3% carbon and extensively used for wide range application due to its flexible property and good combination such as deformable, weldability, and fracture resistance (Krauss, 2015). Low carbon steel which used in manufacturing of machine parts are not subjected to high mechanical stresses, such as shafts, chain links, pins, cemented bushes, gears, flanges and standard screws for low-stress chain drives (Selçuk et al., 2003). In each year, low carbon steel has been used in tonnage for various applications. Structural shapes and beams are produced for buildings and bridges, while plate is produced for line pipe and sheet for automobile. Nowadays, the technologies of construction and automotive are so far beyond, such applications are desired to improve their abilities for handle last longer and safety factors.

Automotive industrial is dramatically increasing the number of developers with highly competitive to leading on new technology. Presently, improvement of desired properties is emphasized on weight reduction for fuel efficiency , and high strength to keep in safety zone for passengers. In these demanding, steel is answered to raise its property nowadays. The average steel usage currently 900 kg per vehicle, compose in three parts, 34% is used in the body structure such as panels, doors and trunk closures with high strength property to absorb energy in the range of crash zone, part of 23% is used casting iron for engine block and machinable carbon steel for the wear resistant

gears, and other 12% is placed in wheels, fuel tank, and breaking system (Kate, 2018). Carbon steel is the major material in the automotive part. Figure 1.1 illustrates the percentage of material usage in automotive light vehicle in north America. Mild steel is the highest material (29%) compared to other materials used in the automotive light vehicle.

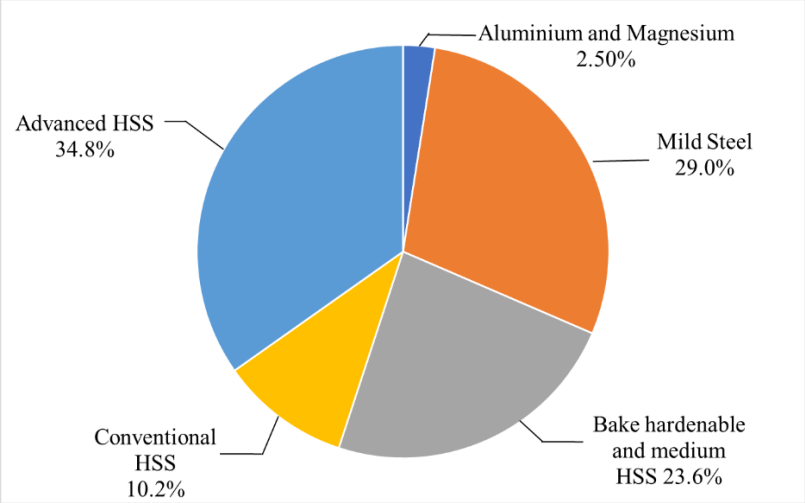

Figure 1.1 Light vehicle metallic material trend in north america (Singh, 2016)

The steel used in the automotive part mostly for the strengtening application and Table 1.1 shows the mechanical properties of various steel and its application. In the body part such as pillar, roof, and floor (Tamarelli, 2011) of automotive required strength in the range above 450 MPa and 23% elongation. This properties is suitable for dual phase and high strength low alloy steel. Common low-strength steel cannot meet the requirements of most manufacturing and production industry in modern society. The research and improvement of low carbon steel has become a vital topic. Thus, to improve low carbon steel properties, various ways were developed to introduce the excellent properties.

Table 1.1 Mechanical properties of various steel and its application (Singh, 2016)

Steel	YS (MPa)	UTS (MPa)	Total EL (%)	Part in automotive
Mild steel	140	270	38-44	A,C,F
Dual phase	280	600	30-34	B
HSLA	350	450	23-27	A,B,S

* A-ancilary part, B-body part, C-closure, F-fuel tank and S-chassis

For example surface properties of carbon steel can be improved by carburizing, carbonitriding or boronizing (Izciler and Tabur, 2006), which enhances the formation of a surface layer that improves properties such as corrosion resistance, wear, and friction. However, these techniques only treat the surface of the material. On the other hand, the bulk properties of carbon steel are modified using the drawing process, which reducing the section of a rod by pulling it through a die (Atienza et al., 2005), that involves with the plastic deformation of the material. In drawing deformation, the hardness and tensile strength of the steel were increased, while impact resistance and ductility were decreased. In addition to the processes mentioned before, modify the steel's properties can be done by other processes with changing its internal structure (ultrafine-grained); this is called, severe plastic deformation (SPD). This process improved both strength and toughness compared with traditional steel. In severe plastic deformation, materials are subjected to reduce the grain sizes in the range of 100-1000 nm. Hence, they are considered as nanostructured materials (Zhu et al., 2004). Among SPD techniques include equal-channel angular pressing (ECAP) (Shin et al., 2002, Matsubara et al., 2003), accumulative roll bonding (ARB) (Tsuji et al., 1999, Saito et al., 1999), mechanical milling (MM) (Belyakov et al., 2003), high-pressure torsion (HPT) (Sabbaghianrad et al., 2012, Ivanisenko et al., 2003, Horita and Langdon, 2005), and cryorolling (Mallick et al., 2017, Roy et al., 2015, Xiong et al., 2018). When

compared to other severe plastic deformation, cryorolling process employ a relatively low accumulated strain which is apply less force to deform the material (Yuan et al., 2018).

Cryorolling is a relatively simple method to produce a UFG structure from its counterpart with lower strains than equal channel angular pressing, high pressure torsion, and accumulative roll bonding, where it involves high strains. This method was originally introduced by Wang et al., (2012). It involves severe cold rolling the material with liquid nitrogen temperature cooling of the materials between consequent rolling passes. Firstly, the sample will undergo a pre-heat treatment process. Initial pre-treatment capable to alter initial microstructure or morphology, relieve internal stresses in the material, dissolution of soluble phases and homogenization of microstructure. There are a few types of initial pre-treatment that have been utilized for steel before cryorolling process such as annealing, quenching, and quenching followed by tempering. After that, the sample is soaked in the liquid nitrogen bath, left for a certain period of time and then carried out rolling process between two rollers.

It has been used to produce a UFG structure in bulk metals and alloys. A wide range of aluminium alloys have been cryorolled (CR) to modify its grain structure from the micrometer regime to the nanometer or submicrometric regime to increase its strength and toughness (Rao et al., 2013). Cryorolling has been achieved on austenite stainless steel (Shi et al., 2017, Mallick et al., 2017, Zheng et al., 2016a, Xiong et al., 2015, Roy et al., 2015), TWIP steel (Klimova et al., 2017), interstitial-free (IF) steel (Sharma et al., 2012), and low carbon steel (Yuan et al., 2018).

The cryorolling process has improved the mechanical due to the effect of grain refinement. Fundamentally, cryorolling process offers the capability of developing grains of UFG sizes in bulk samples. Therefore, grain size can be considered as a key

microstructural factor affecting almost all properties of the mechanical and corrosion behavior of polycrystalline metals.

1.2 Problem statement

Cryorolling has successfully been applied by many researchers for producing ultrafine-grained in other material such as Al (Immanuel et al., 2015, Chandra et al., 2018), Ni (Lee et al., 2005), Cu (Subramanya et al., 2008, Youssef et al., 2011), Ti (Bhaskar et al., 2014, Zherebtsov et al., 2016) and their alloys with the aim of increasing strength. Compared with traditional room temperature rolling, the effect of the grain refinement is greatly improved by cryorolling.

The reports of cryorolling are limited for the nonferrous metals and only a few studies are devoted to the microstructure and mechanical properties of steel and stainless steels after cryorolling. Several researchers (Zheng et al., 2016b, Roy et al., 2015, Kvackaj et al., 2014b)) have investigated the effect of cryorolling on microstructure and mechanical properties of austenite stainless. While Shi et al., (2017) and Zheng et al. (2017) have studied the effect of annealing after cryorolled on microstructure evolution and mechanical properties of austenite stainless. In addition, Sharma et al. (2012) also evaluated the effect of annealing after cryorolling on interstitial-free (IF) steel. Microstructure and texture evolution of high manganese TWIP steel during cryo-rolling was evaluated by Klimova et al. (2017).

The mentioned study above has motivated Yuan et al. (2018) to apply cryorolling process on low carbon steel. They have studied the effect of rolling reduction on microstructure and mechanical properties of low carbon steel with martensite as the initial microstructure. The microstructure evolution and mechanical properties of cryorolled low carbon depend on UFG structure. There are many factors

influenced the formation of UFG such as initial microstructure (pre heat treatment), rolling strain, and post annealing. Due to lack of information on cryorolled low carbon steel, the detail study on parameter affecting the formation of UFG during cryorolling of low carbon steel is needed. Therefore, the present work has been focused to study the effect of pre-heat treatment temperature, thickness reduction, and post-annealing on microstructure, crystallite size, lattice strain, mechanical properties, and corrosion behavior on cryorolled low carbon steel.

1.3 Objectives

The objectives of this research are stated as following:

i. To evaluate the effect of pre-annealing temperature and soaking time on microstructure, crystallite size, lattice strain, microhardness, tensile strength, and fracture morphology of cryorolled low carbon steel.
ii. To investigate the effect of thickness reduction on microstructure, crystallite size, lattice strain, microhardness, tensile strength, fracture morphology, and corrosion behaviour of cryorolled low carbon steel.
iii. To determine the effect of post annealing on microstructure, crystallite size, lattice strain, microhardness, tensile strength, fracture morphology and corrosion behaviour of cryorolled low carbon steel

1.4 Scope of research

The research investigated the effect of cryorolling on low carbon steel. Several major aspects were discussed; preliminary study of initial soaking time in liquid nitrogen, the effect of pre-annealing temperature and soaking time, the effects of different thickness reductions and the effect of post heat treatment temperatures on the properties of cryorolled low carbon steel. The scope of this study covered:

i. The optimum soaking time in liquid nitrogen was studied by austenitizing at 900°C for 60 min, followed by 50% deformation. The ideal soaking time in liquid nitrogen was chosen from the highest value of hardness, ultimate tensile strength, and grain aspect ratio.

ii. The effect of pre-annealing temperature and soaking time on the microstructural evolution, crystallite size, lattice strain, mechanical properties and corrosion behaviour of cryorolled low carbon steel were investigated. The temperatures for pre-annealing are 550°C, 750°C, and 900°C and soaking times are (15, 30, 60, and 120 minutes). The cryorolled samples were investigated by mean of microstructural evolution, X-ray diffraction analysis, mechanical properties, fracture analysis and corrosion behaviour.

iii. The effect of various percentages of thickness reduction was investigated in term of microstructural evolution, crystallite size, lattice strain, mechanical properties, fracture analysis and corrosion behaviour of cryorolled samples. Five percentage of reduction selected are 50%, 60%, 70%, 80%, and 90%.

iv. The effects of post annealing temperature on the microstructural evolution, crystallite size, lattice strain mechanical properties and corrosion behaviour of cryorolled low carbon steel were investigated. The post annealing temperatures selected are 300°C, 350°C, 400°C, and 450°C respectively.

CHAPTER TWO

LITERATURE REVIEW

2.1 Introduction

Low carbon steel is widely used in structural materials but albeit limited to low strain loads. The search for low carbon steel with higher strength to weight ratio is one of the main topics in metal research today. Grain refinement can increase metals strength, as well as improves toughness. Therefore, the grain refinement has been a topic of interest in material engineering science. Currently, there has been an interest to develop ultrafine grain material to achieve high strength and good ductility alloys. For this purpose, several techniques such as severe plastic deformation and advanced thermomechanical process were applied, but cryorolling has been identified as the most potential route for the production of bulk UFG structures with small strain and continuous product.

2.2 Steel

The development of steel starts 4000 years to the beginning of the Iron Age. Steel is harder and stronger than bronze (previously the most widely used metal). This make iron began to displace bronze in weaponry and tools. For the following few thousand years, however, the quality of iron produced would depend as much on the ore available as on the production methods. By the 17th century, iron's properties were well understood, but increasing urbanization in Europe demanded a more versatile structural metal. By the 19^{th} century and 20^{th} century, the amount of iron being consumed was expanding until today in various industries. Steel is used in small part like pin, nuts and bolts, and wire until a large part like constructive product, machine

part, and automotive part, etc. Steel is the alloy of iron and carbon in which the carbon content ranges up to 2 wt.%. The metal alloy can be classified as shown in Figure 2.1.

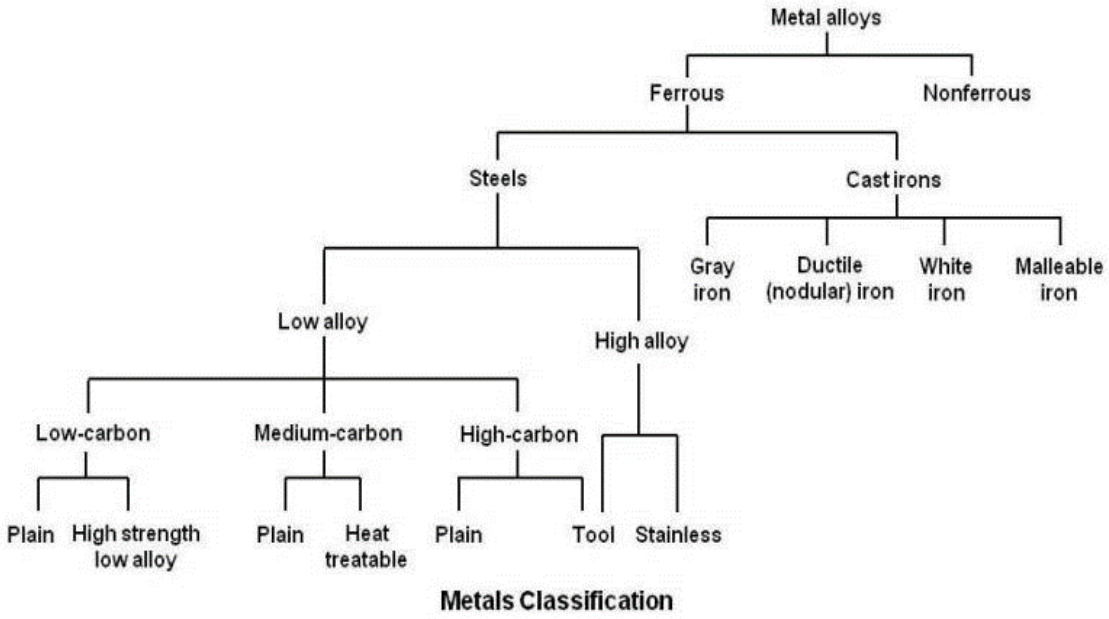

Figure 2.1 Classification of metallic (Shaymaa, 2012)

Alloy steel is steel that is alloyed with a variety of elements in total amounts between 1.0 wt.% and 50 wt.% to improve its mechanical properties. Alloy steels are divided into two groups: low alloy steels and high alloy steels. Alloy steels have definite ranges of carbon and limits on manganese, silicon, copper, phosphorus, and sulfur but may also contain definite ranges or minimum quantities of aluminum, chromium, cobalt, niobium, molybdenum, nickel, titanium, tungsten, vanadium, zirconium, or any other element added to obtain a desired alloying. The alloying elements were added for strength, toughness, hardness, and ductility or machinability (Gouda, 2014).

Low alloy steels also known as carbon steels. Carbon steel contains iron and alloying elements that do not exceed these limit; 1 wt.% carbon, 0.6 wt.% copper, 1.65 wt.% manganese, 0.4 wt.% phosphorus, 0.6 wt.% silicon, and 0.05 wt.% sulfur. The

family of carbon is usually divided into four families; low carbon-steel, medium-carbon steel, high-carbon steel; very-high carbon steel. The low-carbon steel contain less than 0.30 wt.% carbon, the medium-carbon steel has carbon in the range 0.30 to 0.45 wt.% carbon, the high-carbon steel which range from 0.45 to 0.75 wt.% carbon, and the very-high-carbon steels which range up to 1.50 wt.% carbon. The low-carbon steel, often termed “mild” steel is widely used than the grades with higher carbon content. They are ductile, ease to machine or form, and can be welded by any process. As the carbon content increases, tensile strength and hardness increases, but ductility declines, and machining of the steel may become more difficult (ASTM, 2005).

Steels can be cast directly to the desired shape, or ingots which are reheated and hot worked into a wrought shape by extrusion, forging, rolling, or other processes. Wrought steels are the majority engineering material used and have a variety of forms with different finishes and properties. Different types of steel are produced following to the desired properties to appropriate the application, and various coding systems are used to difference type of steels based on these properties.

2.3 Low Carbon Steel (LCS)

Low carbon steel is steels that contain less than 0.3 wt.% of carbon. Microstructures of low carbon steels consist of ferrite and pearlite constituents. Therefore, these alloys are relatively soft and weak but have outstanding ductility and toughness. In addition, LCS are machinable, weldable, and of all steels, are the least expensive to produce. Low carbon steel usually used directly from the forming process, either in hot or cool forming. This is due to the workability and easy to deform. Moreover, low carbon content in low carbon steel, give the best weldability among the steel. Increasing carbon content makes the steel increase in hardness and more prone

to cracking when welded. In term of formability, low carbon steel is easier to form into certain shapes through methods such as pouring, pressing and molding. Low carbon steel is widely used for buildings and bridges (beam), line pipe (plate), and automotive (sheet). These applications are driven by manufacturing requirements for good formability and weldability, and performance requirements of good combinations of strengths and fracture resistance for given applications. Table 2.1 shows the chemical compositions of different types of low carbon steel. The carbon percentage increases in order 1010, 1018, 1020 and 1022. All the steels contain carbon percentage lower than 0.25 wt.% which satisfied the low carbon steel's carbon content.

Table 2.1 Compositions of low carbon steel, mechanical properties, and typical applications for various low carbon steel (Rakhit, 2013, Altan and Tekkaya, 2012)

AISI	**Composition (wt.%)**				**Tensile Strength (MPa)**	**Yield Strength (MPa)**	**Ductility (%EL in 50 mm)**	**Applications**
	C	Mn	P	S				
1010	0.1	0.45	0.04	0.05	325	180	28	Automobile panels, nails and wire, etc.
1018	0.18	0.6	0.04	0.05	440	370	15	gears, pins, dowels, and die sets, etc.
1020	0.2	0.45	0.04	0.05	380	210	25	Pipe, structural and sheet steel, etc.

Higher strengths are increasingly produced in steels with lower carbon contents, an approach that improves formability, weldability, and toughness or fracture resistance. As a result, there have been dramatic and continuous changes in the compositions of low-carbon steels, their strength, ductility, and toughness, and the

processing approaches for their manufacture (Krauss, 2015). Early approaches to design of steel structures involved increasing the section size of low-strength, and increase load-carrying capacity. There are recently approaches for vehicles have been based on developing low-carbon sheet steel microstructures of higher strength to reduce section size and weight in response to powerful economic factors, the need for fuel reduction, and safety concerns.

2.3.1 Phase diagram of steel

Carbon steel composed of varies phases such as ferrite, pearlite, cementite, austenite, and martensite. Each phase has a difference property as depicted in Table 2.2 and difference method to produce it. Low carbon steel contains large fraction of ferrite or alpha (α) which is the crystalline structure of pure iron at room temperature. Heat up steel at higher temperature makes ferrite unstable and then transform into face centered cubic structure or austenite (γ) phases. Determination of temperature of austenite region can be referring to iron-iron carbide phase diagram as illustrate in Figure 2.2. The temperature of austenite region depends on the carbon percentage (Gandy, 2007). According to the phase diagram for 0.06 wt.% carbon steel, the austenite phase is about 880°C - 900°C above A1 line. Cementite is form in the pearlite structure stack in lamella with ferrite when slowly cooled from austenite phase. The amount of cementite present depends on the carbon percentage in steel. Martensite is the phase that involves with cooling method or called quenching. Many types of cooling can be produced martensite, but the microstructure will be differences depend on cooling rate such as room water and ice water, ice water give higher cooling rate. Figure 2.3 shows phase transformation via annealing from austenite region for Fe-Fe_3C phase diagram.

Table 2.2 Phases in iron-iron carbide (Hasan, 2016)

Phase	Description
Ferrite	Ferrite is α-iron (BCC) having not more than 0.025 wt.% carbon in solid solution. It is major constituent in low carbon steels and wrought iron. Its hardness varies from 50 to 100 HV. Its upper tensile strength is about 330 MPa and percentage elongation about 40%. It can be easily cold worked.
Cementite	Cementite is iron carbide, with maximum of 6.67 wt.% carbon. Its upper tensile strength is about 450 MPa and hardness about 695 HV. It is white in color and is brittle. It occurs in steels which have been cooled slowly. It is magnetic below 250°C. In steels containing carbon less than 0.8 wt.% it is present as a component of another constituent, "pearlite". In steels containing more than 0.8 wt.% carbon it exists as a grain boundary film.
Pearlite	Pearlite microstructure consists of alternate laminations of ferrite and cementite. It contains about 0.8 wt.% carbon in iron. It is the strongest constituent of steel. Its hardness is about 180 HV, ultimate tensile strength about 920 MPa and percentage elongation about 5%.
Austenite	Austenite is a solid solution of carbon in γ-iron (FCC) containing a maximum of 2 wt.% carbon at 1130°C. It is tough and non-magnetic. It exists in plain carbon steels

	above upper critical temperature. Elements like chromium and manganese in steel preserve all or some of austenite down to 0°C. Austenite consists of polyhedral grains showing twins.
Martensite	In plain carbon steel, martensite is obtained by quenching from above upper critical temperature (A_3 or A_{cm}). It is the hardest constituent obtained in given steel. It shows a fine needle-like microstructure. Its hardness is about 749 HV. It is unstable and disappears on reheating the steel. It is magnetic and less tough than austenite. It is highly stressed α-iron supersaturated with carbon.

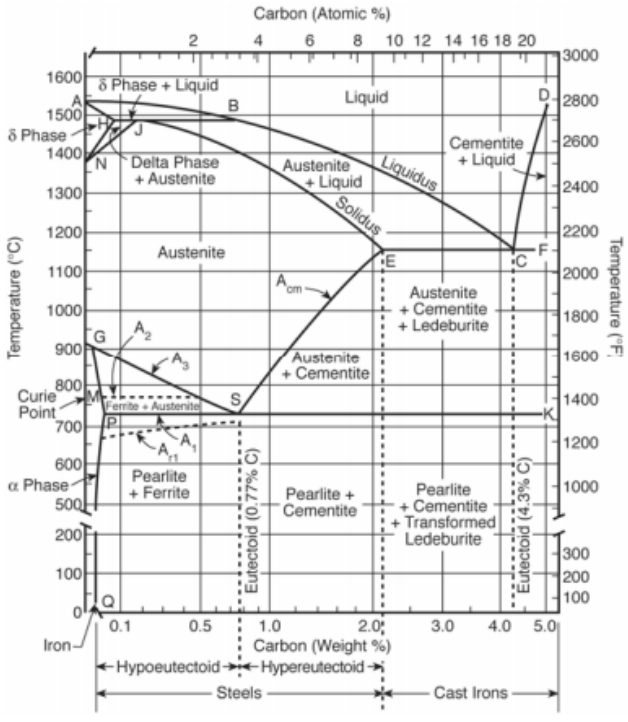

Figure 2.2 Iron-Iron carbide phase diagram (Gandy, 2007)

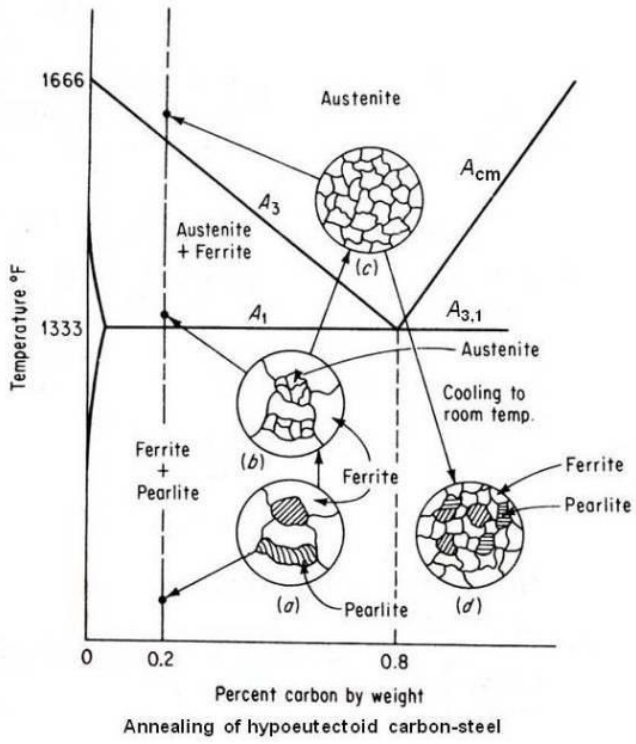

Figure 2.3 Phase transformation via annealing from austenite region (Shah, 2009)

2.4 Strengthening Mechanism

Various type of strengthening mechanisms has been applied, such as grain refining, transformation strengthening, and work hardening. The work hardening was normally applied to strengthen the structural bulk material. The bulk properties of the steel are modified using cold deformation, which involves a plastic deformation of the material. The common cold deformation processes used are drawing, extrusion, rolling etc. After cold deformation, the tensile strength and hardness of the steel increases, while ductility decreases. Rolling is processes which reduced the thickness or change the cross-section of a long work piece by compressive force applied through a set of rollers (Figure 2.4). It is developed in the late 1500s. It is often carried out at elevated temperature first (hot rolling) to change coarse-grained, brittle and porous ingot

structures to wrought structures with finer grain sizes and enhanced properties then followed by cold rolling to get the final thickness required (Dieter, 1988)

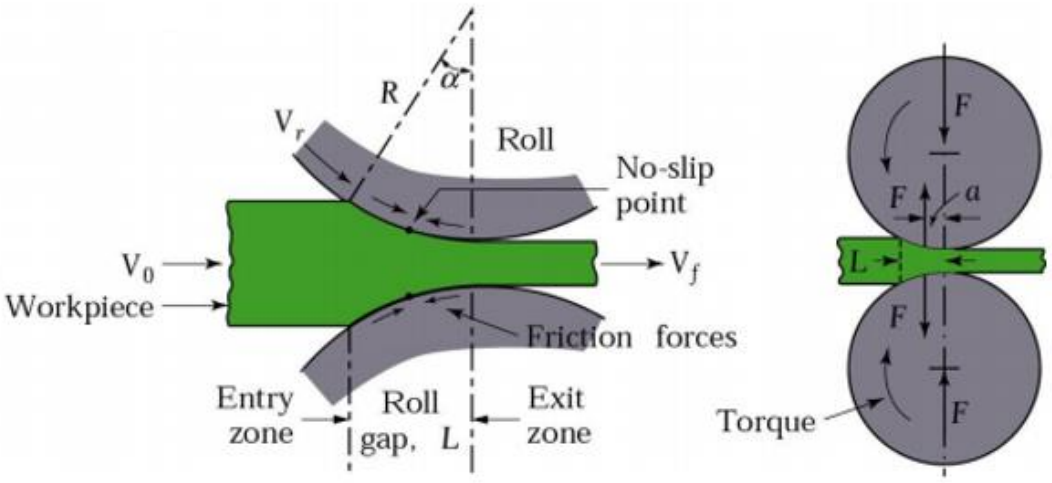

Figure 2.4 Rolling process (Dieter, 1988)

The metal plate is roll within two or more rollers at the normal temperature. The force applied by the roller decrease the thickness of the metal. The grain size was reduced and makes the metal higher in strength. Various studies were carried by many researchers on cold rolling of low carbon steel. A study on the effect of thickness reduction by cold rolling on mechanical properties of low carbon steel was conducted by (Ueji et al., 2004). In their studied, they able to produce ultrafine grain structure of martensite and increased the mechanical properties of the plain low carbon steel at different rolling reduction ranging from 25 to 70% reduction.

In conventional metallurgy such as rolling, forging and extrusion, small grained structures materials are developed through proper thermo-mechanical processing (TMP) methods. The TMP includes both mechanical working and annealing. Karmakar et al. (2013) have report the formation of ultrafine grain by

heating the low carbon steel at the inter-critical of low carbon steel followed by cold work at 80% then annealed 350 °C to 650 °C. The strength after cold increased as compared with as-received but after annealed, the strength slightly dropped and ductility increases. Lei et al. (2010) have obtained ultrafine grain with yield strength in the range 613-647 MPa after cold rolling. Meanwhile Wang et al. (2010) have achieved ultrafine grain when low carbon steel was heated at autenizing temperature (1000°C for 30 min) then cool down to 760°C with 30 min holding time. The sample then immediately quenched to obtain dual-phase structure followed by cold rolled at 64% reduction. Cold rolled sample was then annealed at room temperature for 90 min which resulted in 788 MPa and 17.8% for ultimate tensile strength and elongation. Nevertheless, the TMP has some drawbacks because separate processing routes are required for each different alloy composition and these method yield materials with grain sizes in the range of ~1–10 μm (Langdon, 2007).

In addition to the processes mentioned above, there are other processes that modify the steel's properties by changing its internal structure; this is called, severe plastic deformation (SPD). Currently, it is well known that grain size is the major parameters contribute to the superior mechanical properties especially yield strength and tensile strength. It is well known that yield strength, σ_y, is increased by refining the grain size according to Hall Petch relationship (Huang and Langdon, 2013) as indicated by equation 2.1.

$$\sigma_\gamma = \sigma_o + k_\gamma d^{-1/2} \quad (2.1)$$

Where σ_γ is the yield stress, σ_o is the lattice friction stress, k_γ is a constant of yielding and d is the grain size. Hence, the yield strength of the material increases when the grain size was reduced (Huang and Langdon, 2013, Langdon, 1982).

2.5 Severe Plastic Deformation (SPD)

Severe plastic deformation is defined as intensive plastic straining composed under high pressure. It has received increasing attention due to extremely fine-grained structure and very high strength. The advantage of SPD is the development of materials having good machinability, forgeability and formability at potentially low processing cost. Ultrafine grained materials produced by severe plastic deformation processing usually have dislocation densities, non-equilibrium grain boundaries and other structural features associated with plastic strain. Material possesses an ultrafine grained structure with predominantly high angle grain boundaries and these grain boundaries contain a high density of dislocation indicating their non-equilibrium structure. A lot of researches have shown that ultrafine grain (UFG) can be introduced in wide range of materials from pure metals to alloy, intermetallic compound and metal matrix composite (MMC).

Materials produced by SPD techniques usually have grain sizes in the range of 100–1000 nm. However, they have sub grain structures, such as sub grains, dislocation cells and X-ray coherent diffraction domains (crystallites), which are often smaller than 100 nm. Therefore, they can be called nanostructured materials (Zhu and Langdon, 2004). Ultrafine grain is expected to enhance mechanical properties such as high strength, super-plasticity and low ductile-brittle transition. The materials possess unusual and extraordinary mechanical and physical properties high strength, high toughness at freezing temperature and high-strain rate superplastic behavior

(Bergwerf, 2007). The common SPD processes used for bulk materials include equal-channel angular pressing (ECAP), high-pressure torsion (HPT), and accumulative roll bonding (ARB).

Equal channel angular pressing (ECAP) is one of the processing tools for introducing the grain refinement to the sub-micrometer level in variety types of metals. In ECAP the sample is in the form of rod or bar which is then pressed through a die within a channel that is bent internally through an abrupt angle. The results by experiment shows that after single ECAP pass, the microstructure consists of bands elongated sub-grains and these bands lie oriented parallel to the primary slip system. The high dislocation density is introduced in early stage of straining which leads to formation of inter-granular structure consisting of cells with thick cell walls and low angle misorientation. The thickness of the wall decreases as strain increases by recovery through dislocation annihilation. This will lead to an excess dislocation of only one sign on each boundary and formation of ultrafine grain separated by high-angle non-equilibrium boundaries (Langdon, 2007).

An ultrafine grained low carbon steel was successfully fabricated by (Wang et al., 2005) using equal channel angular pressing (ECAP) at room temperature after pressed to a maximum of 10 passes. The results showed an elongated substructure and increment of tensile strength to 1200 MPa. The ductility of the pressed sample increased after annealing at 500°C for 1 hour. Dong et al. (2002) fabricated ultrafine grained low carbon steel by equal channel angular pressing. Strength after ECAP obtained more than twice increasing from prior operated ECAP. Grain size was reduced to 0.2 – 0.3 μm which considered to be in ultrafine grain region. Meanwhile, Maier al et. (2013) investigated low carbon steel using ECAP. The sample was austenized at 920°C for 30 min followed by quencing then tempered at 670°C for 60

min. Afterward, sample was performed ECAP for six passes along the route which 120° which obtained grain size and hardness of 325 nm and 310 HV.

Compared to ECAP, high-pressure torsion (HPT) processing leads to smaller grain which makes it attractive. The HPT sample is in the form of a thin disk which is placed between two massive anvils. The sample subjected to a pressure, P and then torsional strained through rotation either the lower or upper anvil (Huang and Langdon, 2013). From the HPT process done on Cu-Zn alloy, after ¼ turn, coarse grain is seen in the center of the disk, but a clear grain refinement can be observed near the edge of the disks. After 10 turns, both the center and edge of the disk shows high grain refinement. HPT processing shows the potential for achieving excellent grain refinement (Sabbaghianrad et al., 2014). Effect on microstructure and hardness of AISI 1020 low carbon steel was studied by Marulanda Cardona et al. (2017). A cylindrical sample with 10 mm diameter and 0.8 mm length were tested with high-pressure torsional (HPT). The results show crystallite size decreases with increasing number of turns while the micro strain keeps increasing. After 5 turns, the ferrite and pearlite were in elongated grain shape. The microstructural refinement can be observed as number of turns increases which makes original grain compressed with increasing torsion applied. The hardness results also show an increment in both center and outer region.

Accumulative roll-bonding (ARB) has the ability to produce continuous ultrafine grain sheets in large quantities compared to ECAP and HPT. However, ARB process also has its own weakness which is difficulty to control the bonding quality between two layers after 50% reduction in each pass. A good quality of interface bonding requires a reduction ratio more than 70%. From the study by Sabbaghianrad et al. (2014), they successfully produced ultrafine grain of pure aluminium sheets using

‘four-layer accumulative roll bonding’ (FL-ARB) techniques. The results showed the ability of this technique to produce ultrafine grain at room temperature with good interface bonding strength.

The limitations of SPD processes are it involve great amount of plastic deformation, special procedures, high cost for tooling, complications in design and fabrication of quite small quantities of materials. This limitation has motivated the growing attention in the improvement of other SPD methods such as cryorolling to produce UFG materials which would require less plastic deformation for formation of UFG structure.

2.6 Cryorolling

Cryorolling is the rolling process that carried out at cryogenic temperature (intimately -196°C) by soaking in liquid nitrogen (Figure 2.5). It basically performs to roll like the common rolling process, but the difference is during the cryorolling process, the sample was soaked in the liquid nitrogen for a specific time (depend on the type of materials) prior each strain reduction. Cryorolling has high potential for producing bulk ultra-fine grain materials which can enhance the material properties. The cryogenic rolling deformation requires less plastic deformation achieving ultra-fine grain (UFG) (Stevens, 2007) compare to other severe plastic deformation (SPD) process. In cryorolling, the strain hardening retained up and extent to which rolling ability to carry out which mean that there will be no dislocation annihilation and dynamic recovery during the process. The main advantage of cryorolling is obtaining an ultrafine grain structure. Moreover, handling process of the material is easy in cryorolling compared with other SPD process. A desirable ductility can be achieved if annealing process is done after cryorolling and less plastic deformation required to

achieve ultra-fine grain compared with severe plastic deformation (SPD) (Shivkumar et al., 2016).

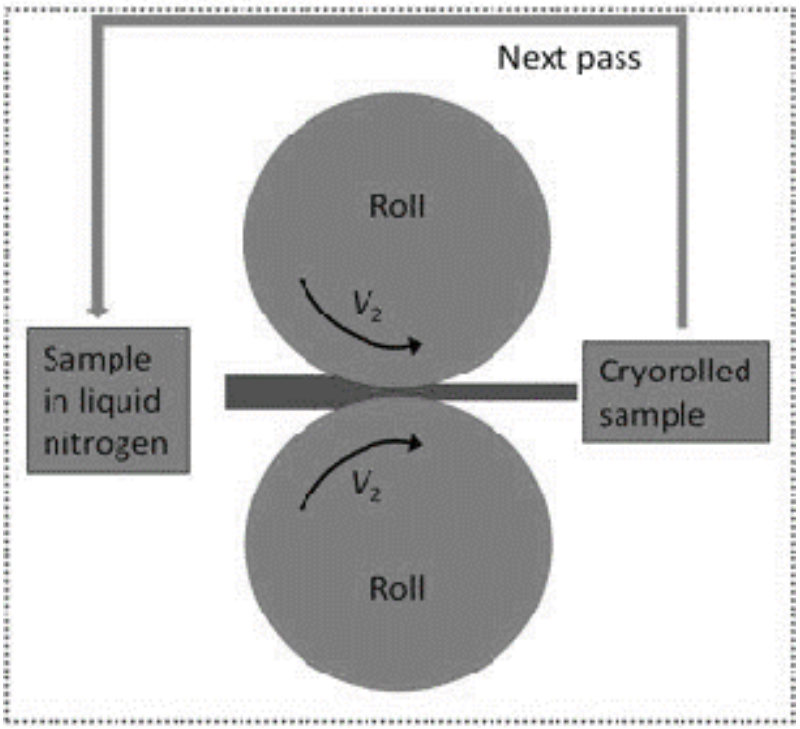

Figure 2.5 Schematic process of cryorolling (Yu et al., 2016)

Cryorolling process is expected to reduce the grain size and generate ultrafine grain with inhibition of dynamic recovery due to cryogenic temperature which can improve strength and hardness of the materials. Mechanism for grain size refinement can be explained based on a model proposed by Mishra et al. (2005) as shown in Figure 2.6. During cryorolling process, the dislocations are not randomly distributed. As the metals under rolling, the dislocation will accumulate at dislocation walls and the regions surrounded by these dislocations wall have relatively low density of dislocation. When the grain deforms as a result of rolling process, the grains subdivided together with dislocation wall act as barriers to dislocation movement. As

deformation proceeds, the sub-grains progressively change into grain boundaries. These elongated sub-grains plastically deformed causing further break-up and formed equiaxed micro grains.

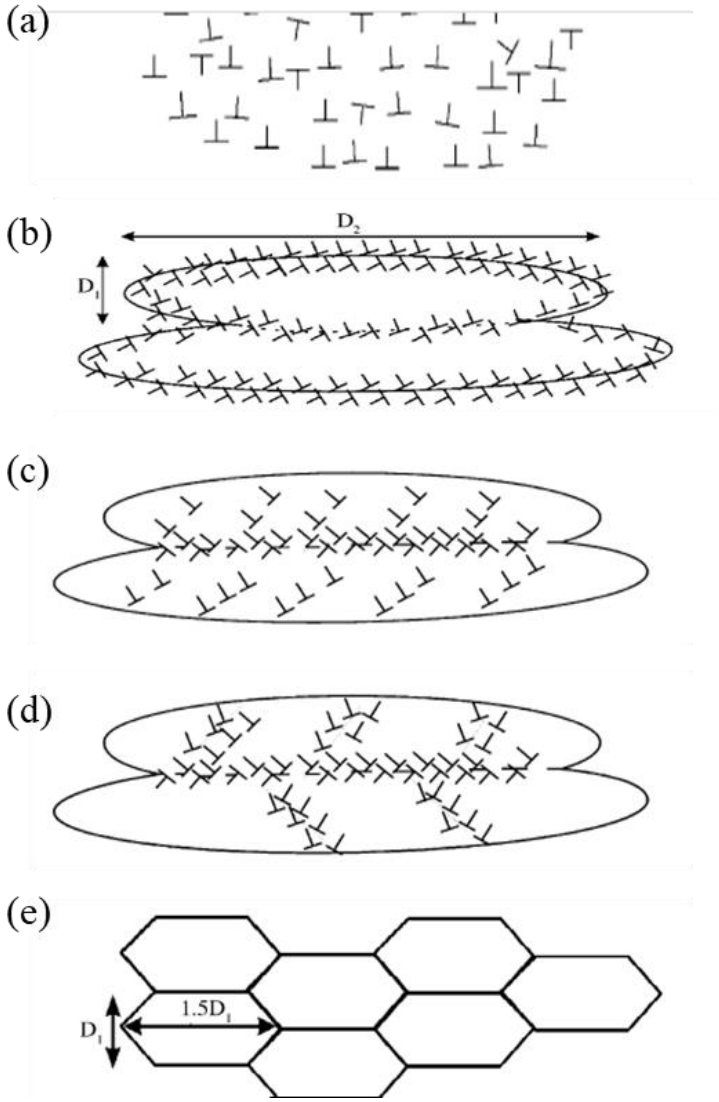

Figure 2.6 Schematic diagram of microstructural evolution occur during severe plastic deformation. (a) homogeneous distribution of dislocation, (b) elongated cell formation, (c) dislocation obstructed by sub-grain boundaries, (d) destruction of elongated sub-grains and (e) reorientation of sub-grain boundaries and development of UFG structures (Mishra et al., 2005)

Several studies have successfully produced ultrafine grained for stainless steel (Xiong et al., 2017), aluminium alloy (Abbasi-Baharanchi et al., 2017), copper alloy (Zhang et al., 2017) and titanium alloy (Zherebtsov et al., 2013). Xiong et al. (2018) have produced nano-grained in 316LN austenitic stainless steel during cryorolling. This has led to improvement in strength and hardness. At 90% reduction, the yield strength, ultimate tensile strength, and microhardness increase from 209 MPa, 527 MPa and 170HV (as received material) to 1468 MPa, 1572 MPa, and 528 HV respectively. Abbasi-Baharanchi et al. (2017) evaluated the nanostructured of Al 6061 alloy by cryorolling. A nanostructured Al6061 alloy with grain size of 61 nm was produced by cryorolling process with hardness of 118 HV. Figure 2.7 shows the engineering stress-strain curves of Al6061 alloy in different conditions, including solution treated (ST), T6 heat treated (T6), cryorolled (CR) and peak aged after cryroll (CR+PA) samples. The strength of the CR sample (σy=(271±16) MPa and σUTS=(297±18) MPa) was much higher than that of ST sample (σy=(50±6) MPa and σUTS=(134±10) MPa). This is due to the high density of dislocation accumulated as a result of plastic deformation at −196 °C temperature in deformation at cryogenic temperatures. In addition Zhang et al. (2017) reported the improvement in tensile strength for Cu-Cr-Zr alloy with value of 690.13 MPa after cryorolling due to grain refinement. Zherebtsov et al. (2013) claimed the formation nanostructures in pure titanium with grain size of 80-200 nm and ultimate strength of 900 to 1100 MPa.